MATRIX CRACK INTERACTION IN A FIBER-REINFORCED BRITTLE MATRIX COMPOSITE

A. C. WIJEYEWICKREMA and L. M. KEER

Department of Civil Engineering, Northwestern University, Evanston, IL 60201, U.S.A.

Abstract—Multiple cracking in a fiber-reinforced brittle matrix composite under longitudinal tensile loading is investigated within the framework of linear elastic fracture mechanics. A perfect bond is assumed at the interface. Stress intensity factors are presented for different ratios of shear moduli, crack spacings and fiber volume fractions. Stress fields are given for a brittle matrix fiber-reinforced composite, calcium aluminosilicate glass ceramic reinforced with silicon carbide fibers (SiC/CAS). The stress fields are used to predict damage mechanisms in the composite. It is shown that crack interaction effects are significant for crack spacings that are observed in composites with good bonding at the fiber-matrix interface.

INTRODUCTION

Experiments carried out on fiber-reinforced brittle matrix composites have shown that prior to complete failure multiple transverse matrix cracking occurs under longitudinal tensile loading (Evans and Marshall, 1989; Daniel *et al.*, 1989). It has been observed that while the number of cracks increases (reducing the spacing between cracks) there is a saturation density of cracks and hence a minimum crack spacing. The main objective of this paper is to investigate the effect of crack spacing and fiber volume ratio on the crack tip stress intensity factor and the stress fields in the brittle matrix. The stress fields in the brittle matrix are used to predict damage mechanisms in the composite.

Most of the models adopted by various researchers include various assumptions to simplify the analyses. The paper by McCartney (1989) reviews some of the earlier work done in analyzing fracture in brittle matrix composites. To systematically tackle the problem of fracture in brittle-matrix fiber-reinforced composites using a fracture mechanics approach, Wijeyewickrema *et al.* (1991) first considered the case of an annular matrix crack surrounding a single fiber. Next a hexagonal array of fibers was modeled using the concentric circular cylinders model (Wijeyewickrema and Keer, 1991). In that analysis cracking was confined to a single transverse cross-section. In the present paper multiple cracking of the brittle matrix is investigated.

Multiple parallel cracks were first considered by Collins (1962), who considered penny-shaped cracks in an infinite elastic solid. Other previous studies of multiple parallel cracks have been limited to planar problems of a single homogeneous solid. Benthem and Koiter (1973) used an asymptotic approximation method to consider the case of a half-plane with a periodic array of edge cracks while Bowie (1973) used a technique involving conformal mapping to study the same problem. The problem of thermally induced parallel edge cracks in a half-plane was considered by Nemat-Nasser *et al.* (1978) while both edge and internal periodic cracks in a half-plane have been investigated by Nied (1987).

FORMULATION OF THE PROBLEM

The concentric cylinders model used to analyze multiple cracking in a brittle-matrix composite with a hexagonal array of fibers is shown in Fig. 1. Perfect bonding is assumed at the interface of the infinitely long elastic fiber of radius a and the elastic matrix which has an outer radius b. The periodic array of annular cracks which have inner and outer radii of c and d respectively $(a \leqslant c < b, \ a < d \leqslant b)$, are distributed along the z-axis a distance h apart. A uniform longitudinal tensile strain ε_0 is applied to the system at $z = \pm \infty$.
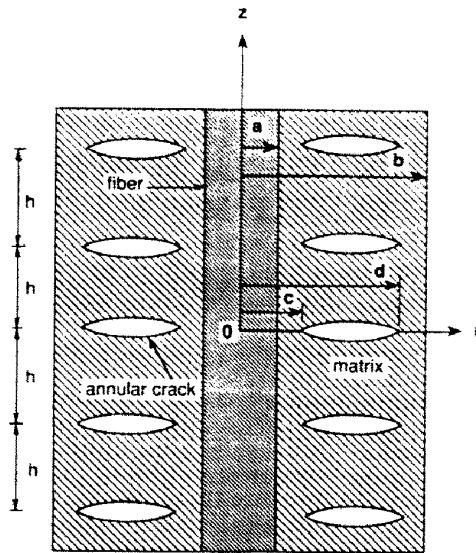
Fig. 1. A periodic array of annular matrix cracks surrounding the elastic fiber. The concentric circular cylinders model represents a unit cell which models the case of a hexagonal array of fibers.

The solution to the multiple cracking problem is obtained by the superposition of the solutions of two related problems: A crack-free uniaxially loaded composite specimen which has a stress-free outer boundary and a matrix cracked specimen loaded only on the crack surfaces which has a zero radial displacement at the outer boundary. The reasons for selecting these boundary conditions have been given elsewhere (Wijeyewickrema and Keer, 1991) and will not be repeated here. The self-equilibrating stresses applied to the crack surfaces in the second problem are equal and opposite to the stresses $\sigma_{zz}^1(r)$ obtained from the undamaged composite specimen.

The multiple crack problem is tackled by making use of the stress field developed previously for a single crack by Wijeyewickrema and Keer (1991). Since $z = 0$ is a plane of symmetry only the upper half of the representative cell $z \geq 0$ is considered. In what follows, the superscripts and subscripts 0 and 1 refer to the fiber and matrix, respectively. Love's stress functions $\chi^0(r, z)$ and $\chi^1(r, z)$ for the fiber and matrix respectively are given by

$$\chi^0(r, z) = \frac{2}{\pi} \int_0^\infty [f_1(s)I_0(rs) + f_2(s)rsI_1(rs)] \sin(zs)\, ds + \int_0^\infty f_3(p)p(2v_0 + zp)\, e^{-zp}J_0(rp)\, dp$$

$$(1)$$

$$\chi^1(r, z) = \frac{2}{\pi} \int_0^\infty [f_4(s)I_0(rs) + f_5(s)rsI_1(rs) + f_6(s)K_0(rs) + f_7(s)rsK_1(rs)] \sin(zs)\, ds$$

$$+ \int_0^\infty f_8(p)p(2v_1 + zp)\, e^{-zp}J_0(rp)\, dp, \quad (2)$$

where f_i ($i = 1, \ldots, 8$) are unknown functions, $J_n(\ )$ is the Bessel function of the first kind of order n and $I_n(\ )$ and $K_n(\ )$ are the modified Bessel functions of the first and second kind respectively of order n. The Poisson ratios are denoted by v_i, ($i = 0, 1$). The complete displacement and stress fields for the fiber and matrix are given by eqns (2)–(6) and (8)–(12) in Wijeyewickrema and Keer (1991). The axial stress in the matrix $\sigma_{zz}^1(r, z)$ is given by

$$\sigma_{zz}^1(r,z) = \frac{2}{\pi} \int_0^\infty \{f_4(s)I_0(rs) + f_5(s)[2(2-v_1)I_0(rs) + rsI_1(rs)] + f_6(s)K_0(rs)$$

$$+ f_7(s)[-2(2-v_1)K_0(rs) + rsK_1(rs)]\}s^3 \cos(zs) \, ds + \int_0^\infty f_8(p)p^4(1+zp) \, e^{-zp}J_0(rp) \, dp.$$

$$(3)$$

The continuity conditions at the interface due to the assumed perfect bond are

$$u_r^0(a,z) = u_r^1(a,z), \quad u_z^0(a,z) = u_z^1(a,z), \quad 0 \leqslant z < \infty, \tag{4}$$

$$\sigma_{rr}^0(a,z) = \sigma_{rr}^1(a,z), \quad \sigma_{rz}^0(a,z) = \sigma_{rz}^1(a,z), \quad 0 \leqslant z < \infty. \tag{5}$$

The boundary conditions on the external cylindrical surface of the matrix are given by

$$u_r^1(b,z) = 0, \quad 0 \leqslant z < \infty, \tag{6}$$

$$\sigma_{rz}^1(b,z) = 0, \quad 0 \leqslant z < \infty, \tag{7}$$

and the conditions on the planes of symmetry are

$$u_z^0(r,nh) = 0, \quad 0 \leqslant r \leqslant a, \quad u_z^1(r,nh) = 0, \quad a \leqslant r < c, \quad d < r \leqslant b, \tag{8}$$

$$\sigma_{rz}^0(r,nh) = 0, \quad 0 \leqslant r \leqslant a, \quad \sigma_{rz}^1(r,nh) = 0, \quad a \leqslant r \leqslant b, \tag{9}$$

$$\sigma_{zz}^1(r,nh) = -p(r), \quad c < r < d, \tag{10}$$

where $n = -\infty, \ldots, +\infty$. Here $p(r)$ is the axial stress in the matrix in an undamaged composite subjected to uniform longitudinal tensile strain at $z = \pm\infty$.

Equation (8a) yields the condition $f_3(p) = 0$, while from the expressions for shear stress and the antisymmetric nature of this stress it can be shown that eqn (9) is satisfied.

By defining a new unknown function $\phi(r)$ which is related to the gradient of the crack opening displacement as follows:

$$\frac{\mu_1}{1-v_1} \frac{\partial}{\partial r} u_z^1(r,0) = \phi(r), \quad c < r < d, \tag{11}$$

it can be shown from eqns (8b) and (11) that

$$p^3 f_8(p) = \int_c^d t\phi(t)J_1(pt) \, dt. \tag{12}$$

From the four boundary conditions at the interface and the two conditions on the external surface of the matrix a system of six equations is obtained and the unknown functions f_i, $(i = 1, 2, 4, 5, 6, 7)$ can be expressed as

$$f_i(s) = \int_c^d t\phi(t) \, dt \frac{1}{s^3} \sum_{j=1}^6 \frac{A_{ij}(s)h_j(t,s)}{\Delta(s)} \tag{13}$$

where $\Delta(s)$ is the determinant and $A_{ij}(s)$, $(i = 1, 2, 4, 5, 6, 7; j = 1, \ldots, 6)$ are the appropriate elements of the adjoint of the coefficient matrix of the system of six equations. The functions $h_j(t,s)$, $(j = 1, \ldots, 6)$ are given by eqns (28)–(33) in Wijeyewickrema and Keer (1991). By substituting for f_i, $(i = 4, \ldots, 8)$ from eqns (12) and (13) into eqn (3), the stress $\sigma_{zz}^1(r,z)$ at

any point (r, z) in the matrix on the upper part of the concentric cylinder due to a single crack located at $z = 0$, is obtained as

$$\sigma^1_{zz}(r,z) = \frac{2}{\pi} \int_c^d t\phi(t)\, dt \int_0^x ds \bar{k}_2(r,t,s) \cos(zs) + \int_c^d tM(r,t,z)\phi(t)\, dt \tag{14}$$

where

$$\bar{k}_2(r,t,s) = \frac{1}{\Delta(s)} \left\{ \left(\sum_{i=1}^{6} A_{4i}h_i \right) I_0(rs) + \left(\sum_{i=1}^{6} A_{5i}h_i \right) (2(2-v_1)I_0(rs) + rsI_1(rs)) \right.$$

$$\left. + \left(\sum_{i=1}^{6} A_{6i}h_i \right) K_0(rs) + \left(\sum_{i=1}^{6} A_{7i}h_i \right) (-2(2-v_1)K_0(rs) + rsK_1(rs)) \right\} \tag{15}$$

and

$$M(r,t,z) = \frac{1}{t\pi[(t+r)^2 + z^2]^{1/2}} \left\{ \frac{E(k)}{(t-r)^2 + z^2} \right.$$

$$\times \left[(t^2 - r^2 - z^2) + \frac{z^2[(t^2 - r^2)(7t^2 + r^2) + z^2(6t^2 - 2r^2 - z^2)]}{[(t+r)^2 + z^2][(t-r)^2 + z^2]} \right]$$

$$\left. + K(k) \left[1 - \frac{z^2(t^2 - r^2 - z^2)}{[(t+r)^2 + z^2][(t-r)^2 + z^2]} \right] \right\}. \tag{16}$$

$$k^2 = \frac{4tr}{(t+r)^2 + z^2} \tag{17}$$

here $K(k)$ and $E(k)$ are complete elliptic integrals of the first and second kind respectively.

By using the principle of superposition, the axial stress in the matrix on the $z = 0$ plane due to the cracks located in the upper part of the cylinder ($z > 0$) is obtained from eqn (14) by setting $z = nh$ and summing on n from $+1$ to ∞. From symmetry considerations the axial stress in the matrix on the $z = 0$ plane due to cracks located in the lower part of the cylinder ($z < 0$) is the same as the effect of the cracks located on the upper part of the cylinder. Hence the axial stress $\sigma^{1a}_{zz}(z, 0)$ on the $z = 0$ plane due to all the cracks except the central crack (located on the $z = 0$ plane) is

$$\sigma^{1a}_{zz}(r,0) = 2 \int_c^d t\phi(t)K_2(r,t)\, dt, \tag{18}$$

where

$$K_2(r,t) = \frac{2}{\pi} \int_0^\infty ds \bar{k}_2(r,t,s) \sum_{n=1}^{\infty} \cos(nhs) + \sum_{n=1}^{\infty} M(r,t,nh). \tag{19}$$

The axial stress $\sigma^{1b}_{zz}(r, 0)$ on the $z = 0$ plane due to the central crack is

$$\sigma^{1b}_{zz}(r,0) = \frac{1}{\pi} \int_c^d \left\{ \frac{1}{t-r} + k(r,t) \right\} \phi(t)\, dt, \tag{20}$$

where

$$k(r, t) = k_1(r, t) + 2tk_2(r, t), \tag{21}$$

$$k_1(r, t) = \frac{m(r, t) - 1}{t - r} + \frac{m(r, t)}{t + r}, \tag{22}$$

$$m(r, t) = \begin{cases} E(r/t), & r < t \\ \dfrac{r}{t} E(t/r) + \dfrac{t^2 - r^2}{rt} K(t/r), & r > t \end{cases} \tag{23}$$

$$k_2(r, t) = \int_0^\infty \overline{k_2}(r, t, s)\, \mathrm{d}s. \tag{24}$$

Hence the axial stress on the $z = 0$ plane due to all the cracks is

$$\sigma_{zz}^1(r, 0) = \frac{1}{\pi} \int_c^d \left\{ \frac{1}{t - r} + k(r, t) + 2\pi t K_2(r, t) \right\} \phi(t)\, \mathrm{d}t \tag{25}$$

and from eqns (25) and (10) the required integral equation is obtained as

$$\frac{1}{\pi} \int_c^d \left\{ \frac{1}{t - r} + l(r, t) \right\} \phi(t)\, \mathrm{d}t = -p(r), \quad c < r < d, \tag{26}$$

where

$$l(r, t) = k(r, t) + 2\pi t K_2(r, t). \tag{27}$$

When the crack tips c and d are embedded in the matrix, eqn (26) is solved with the condition that the crack tips are closed at c and d, given by

$$\int_c^d \phi(r)\, \mathrm{d}r = 0. \tag{28}$$

Although four different cases can be considered depending on where the crack tips are located, here attention is focused on the fully cracked matrix, i.e. when $c = a$ and $d = b$.

The solution of the integral equation which has a generalized Cauchy kernel is of the form

$$\phi(t) = (t - a)^\beta g(t), \quad a < t < b \tag{29}$$

where it is noted that $\phi(t)$ is bounded at $t = b$. The characteristic equation required to determine β is obtained by applying the function-theoretic method to the integral equation and is given by eqn (64) in Wijeyewickrema and Keer (1991). The constant β is real and is a function of the material properties of the fiber and matrix. Next, the limits of the integral equation are normalized by defining

$$t = \frac{b - a}{2} \tau + \frac{b + a}{2}, \quad r = \frac{b - a}{2} \rho + \frac{b + a}{2}, \tag{30}$$

$$\phi(t) = (1 - \tau)^{-1/2} (\tau + 1)^\beta F(\tau), \tag{31}$$

$$p(r) = P(\rho), \quad L(\rho, \tau) = \frac{b-a}{2} l(r, t),$$
(32)

to obtain the equation

$$\frac{1}{\pi} \int_{-1}^{+1} \left\{ \frac{1}{\tau - \rho} + L(\rho, \tau) \right\} F(\tau)(1-\tau)^{-1/2}(\tau+1)^{\beta} \, d\tau = -P(\rho), \quad -1 < \rho < +1.$$
(33)

Equation (33) is solved together with the additional condition $F(+1) = 0$, to account for the boundedness of $\phi(t)$ at $t = b$ by using a Gauss–Jacobi type quadrature formula (Erdogan et al., 1973).

The mode I stress intensity factor at the crack tip a is defined by

$$K(a) = \lim_{r \to a} 2^{1/2}(a-r)^{-\beta} \sigma_{zz}^{0}(r, 0),$$
(34)

and is expressed as

$$K(a) = \mu^{*} \lim_{r \to a} 2^{1/2}(r-a)^{-\beta} \phi(r) = \mu^{*} a_{0}^{-\beta} F(-1)$$
(35)

where

$$\mu^{*} = \frac{\bar{\mu}(1+\kappa_{1})}{2} \left\{ \frac{(3+2\beta)(1+\bar{\mu}\kappa_{1}) - (1+2\beta)(\bar{\mu}+\kappa_{0})}{(\bar{\mu}+\kappa_{0})(1+\bar{\mu}\kappa_{1}) \sin \pi(1+\beta)} \right\}.$$
(36)

Here $\bar{\mu} = \mu_{0}/\mu_{1}$ where μ_{i}, $(i = 0, 1)$ are the shear moduli, $\kappa_{i} = 3 - 4v_{i}$, $(i = 0, 1)$ and $a_{0} = (b-a)/2$. The compact formula given by Krenk (1975) is used to obtain $F(-1)$. The infinite series in eqn (19) are evaluated by truncating the series such that the desired accuracy is obtained. When the crack spacing $h/2a = 0.01$, it was found that summing the infinite series in eqn (19) up to $n = 50$ was sufficient.

RESULTS AND DISCUSSION

Numerical results are given for the stress intensity factors at the crack tip, interfacial stresses and the axial stresses in the composite at different locations. In all the numerical examples the Poisson ratios were taken as $v_{0} = v_{1} = 0.25$ and $p(r) = \sigma_{zz}^{1}(r) = \sigma_{0}$. The axial stress in the matrix σ_{0} is obtained by considering an undamaged concentric circular cylinders model which is subjected to a uniform longitudinal tensile strain ε_{0} at $z = \pm \infty$. When the outer matrix surface is stress free

$$\sigma_{0} = E_{1}\varepsilon_{0} - 2v_{1}\sigma^{*} \left(\frac{a^{2}}{b^{2} - a^{2}} \right),$$
(37)

where

$$\sigma^{*} = \frac{2\varepsilon_{0}(v_{0} - v_{1})V_{m}}{V_{f}/k_{p1} + V_{m}/k_{p0} + 1/\mu_{1}},$$
(38)

and $V_{f} = a^{2}/b^{2}$, $V_{m} = 1 - V_{f}$ and $k_{pi} = \mu_{i}/(1 - 2v_{i})$, $(i = 0, 1)$. (Appendix A, Wijeyewickrema and Keer, 1991.) Here μ, v and E are the shear modulus Poisson ratio and Young's modulus respectively and the subscripts 0 and 1 refer to the fiber and matrix. Motivated by experiments carried out at Northwestern University, the stress fields are presented for a calcium aluminosilicate glass ceramic reinforced with Silicon Carbide fibers (SiC/CAS). The SiC/CAS composite has the following material properties (Daniel et al., 1989):
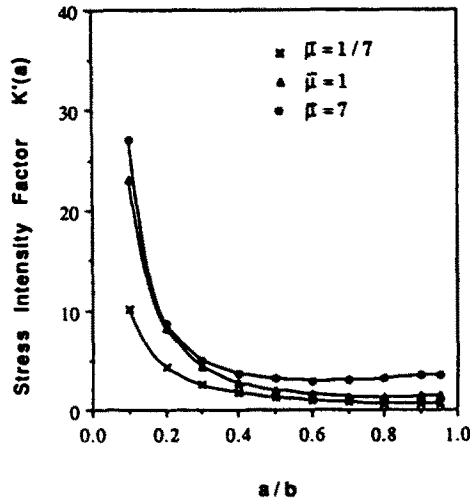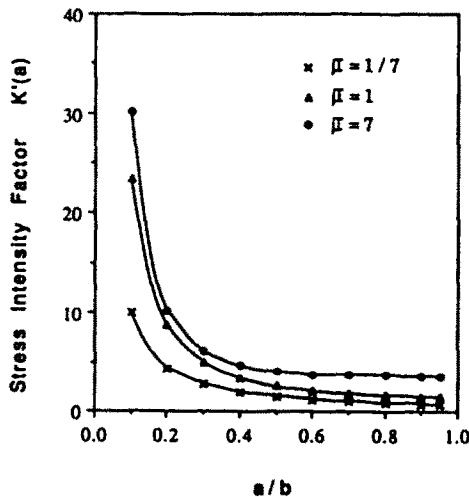
Fig. 2. Stress intensity factors for annular edge cracks when the matrix is fully cracked, crack spacing $h/b = 0.5$.

$$E_0 = 207 \text{ GPa } (30.0 \times 10^6 \text{ psi}), \quad E_1 = 98 \text{ GPa } (14.2 \times 10^6 \text{ psi}),$$

$$v_0 = v_1 = 0.25, \qquad V_f = 0.4. \tag{39}$$

For these material values $\bar{\mu} = 2.1127$, $a/b = 0.6325$ and $\beta = -0.4242$. All results for the stresses are normalized with respect to the uncracked matrix stress σ_0, i.e. $\bar{\sigma}_{rr}(a, z) = \sigma_{rr}(a, z)/\sigma_0$ etc.

The normalized stress intensity factor is defined by

$$K'(a) = \frac{K(a)}{\sigma_0 a_0^{-\beta}} = \mu^* F(-1). \tag{40}$$

The crack tip singularity $-\beta$ depends on $\bar{\mu}$ and for $\bar{\mu} = 7$, 1 and $1/7$ takes values of $+0.3304$, $+0.5$ and $+0.7149$ respectively. As the stiffness of the fiber increases the crack tip singularity $-\beta$ decreases. It is not possible to compare $K'(a)$ for different ratios of $\bar{\mu}$ since the crack tip singularity at a is dependent on $\bar{\mu}$. In Figs 2 and 3 the normalized stress intensity factors

Fig. 3. Stress intensity factors for annular edge cracks when the matrix is fully cracked, crack spacing $h/b = 1.0$.
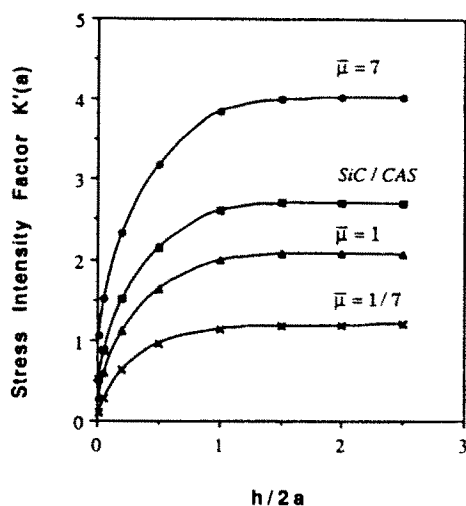
Fig. 4. Stress intensity factors for annular edge cracks when the matrix is fully cracked, fiber volume fraction $V_f = 0.4$.

are plotted against a/b for crack spacings of $h/b = 0.5$ and 1.0, respectively. When the radius of the fiber increases $K'(a)$ decreases monotonically when $h/b = 1.0$, but when $h/b = 0.5$, $K'(a)$ initially starts decreasing but starts to increase as $a/b \to 1.0$. In Figs 4 and 5 the normalized stress intensity factor is plotted against $h/2a$ for fiber volume fractions of $V_f = 0.4$ and 0.6, respectively. The mid-planes between cracks act as constraining boundaries with no axial displacements. When the crack spacing $h/2a \to 0$, this boundary effect results in $K'(a) \to 0$. For the smaller volume fraction of $V_f = 0.4$, $K'(a)$ has no significant change for $\bar{\mu} > 1$ when the crack spacing $h/2a > 2.0$. For the larger volume fraction $V_f = 0.6$, for $\bar{\mu} > 1$, $K'(a)$ is constant when $h/2a > 1.0$ and for $\bar{\mu} \leqslant 1$, $K'(a)$ is constant when $h/2a > 1.5$. Hence it can be concluded that for stiff fibers when the fiber volume fraction is large, cracks can be spaced as close as one fiber diameter apart with no crack interaction effects. Experimental results (Daniel *et al.*, 1989) indicate that for a SiC/CAS composite which has a good bond at the interface, the minimum crack spacing is about two fiber diameters. From Fig. 4 it is seen that crack interaction effects are significant for the SiC/CAS composite only when the crack spacing is smaller than two fiber diameters. It is noted that the assumption
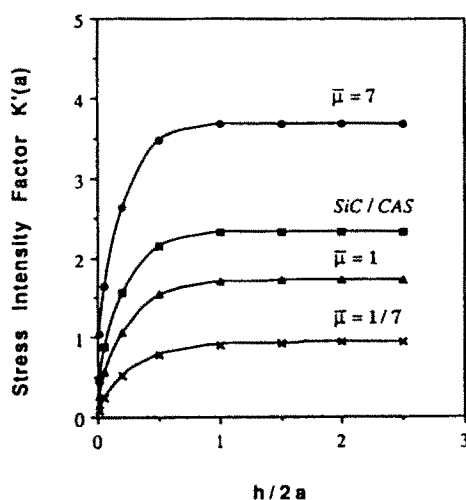

Fig. 5. Stress intensity factors for annular edge cracks when the matrix is fully cracked, fiber volume fraction $V_f = 0.6$.
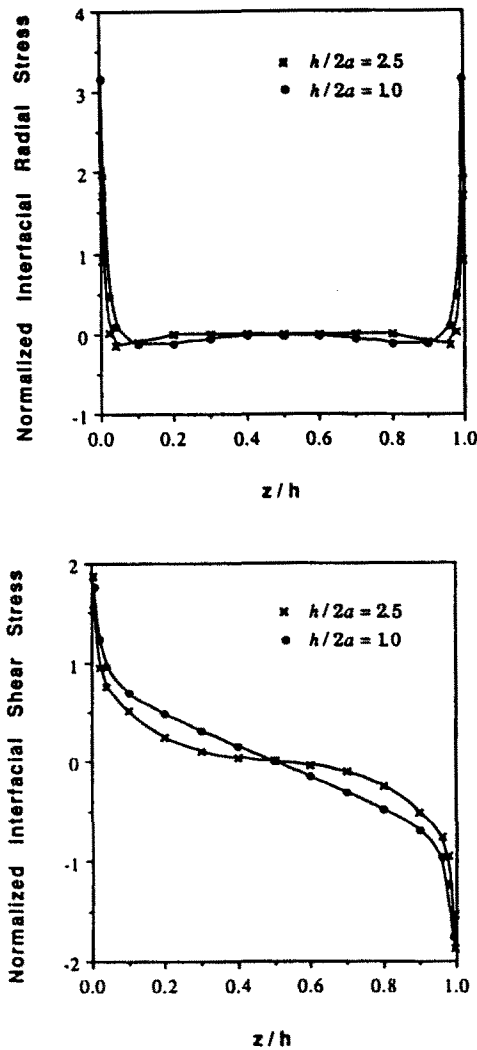
Fig. 6. Normalized interfacial stresses of the SiC/CAS composite for different crack spacings.

of perfect bonding at the interface made in the analysis, theoretically permits the number of cracks that are generated to keep on increasing without any limit and hence it is not possible to predict a minimum crack spacing. As will be shown later, the interfacial shear stresses near the crack increase relative to the matrix axial stresses when the crack spacing decreases, thereby causing the dominant failure to become interfacial rather than in the matrix for small spacings.

The interfacial stresses are given in Fig. 6, where both $\bar{\sigma}_{rr}(a, z)$ and $\bar{\sigma}_{rz}(a, z)$ are singular when approaching the crack planes. Due to the opening up of the cracks $\bar{\sigma}_{rr}(a, z)$ decreases rapidly and changes to compression. The tensile radial stresses near the crack planes will lead to interfacial debonding. The shear stresses drop to zero at the mid-plane between cracks due to symmetry considerations. The high shear stresses will facilitate relative slip between the fiber and the matrix after interfacial debonding has taken place. The axial stress distribution in the fiber at the crack plane $\bar{\sigma}_{zz}(r, 0)$, given in Fig. 7 shows that when the crack spacing gets smaller the axial stress in the center of the fiber starts increasing while decreasing in the vicinity of the interface.

In Fig. 8 the axial stress at the mid-plane between cracks is plotted for various crack spacings. For a given crack spacing the matrix carries more load at the interface than at the mid-surface between fibers since the load is transferred to the matrix through the interface. For small crack spacings a large drop in axial stress occurs when $r = b$. From Fig. 9 it is seen that the matrix axial stress at the interface is a minimum at the mid-plane
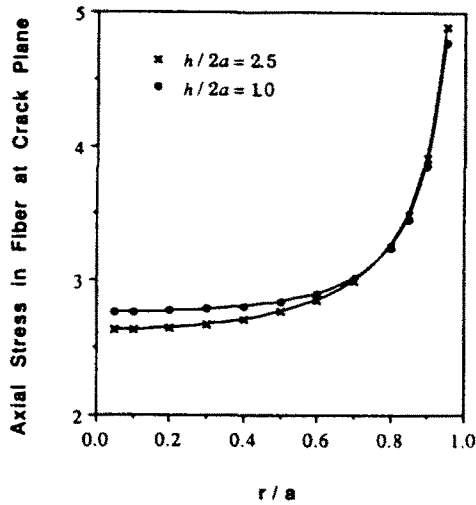
Fig. 7. Normalized axial stress in the fiber on the crack plane of the SiC/CAS composite for different crack spacings.

between cracks. It appears that the high radial and shear interfacial stresses may lead to debonding and relative slip at the interface starting at the crack planes; the crack tip is no longer closed but is blunted, thereby causing the high axial stress near the crack plane to diminish. Hence the axial stress distribution at the interface should be such that it is zero at the crack plane, and reaches a maximum away from the crack plane. To locate the slip region and the position where the maximum axial stress occurs requires an analysis which also incorporates slip at the interface.

Furthermore, Fig. 8 shows that the shear lag theories and other approximate methods used by many investigators, may not provide good results as the spacing becomes smaller, since crack interaction may cause the assumptions that result in uniform axial stresses in the matrix in the radial direction to be invalid. A calculation verifying approximate analyses by the more exacting theory incorporating debonding and slip is preferred.

Figure 10 shows the matrix axial stress at $r = b$ i.e. at the mid-surface between fibers. When the crack spacing becomes smaller, less load is seen to be transferred to the matrix through the interface.
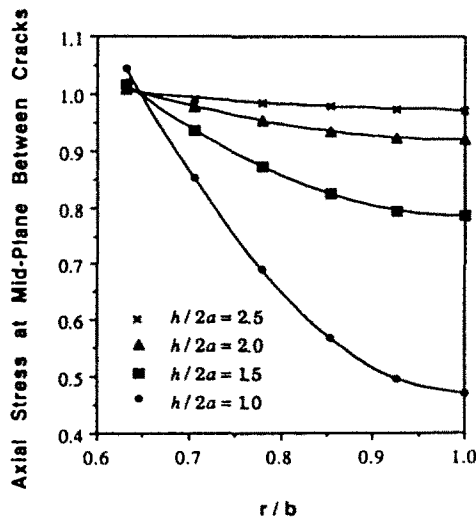

Fig. 8. Normalized axial stress in the matrix at mid-plane between cracks of the SiC/CAS composite for different crack spacings.
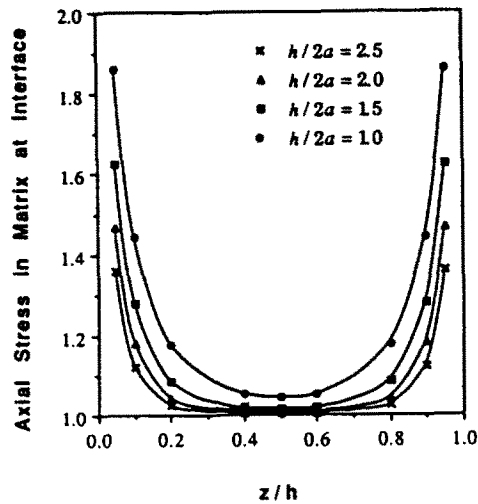
Fig. 9. Normalized axial stress in the matrix at the interface of the SiC/CAS composite for different crack spacings.
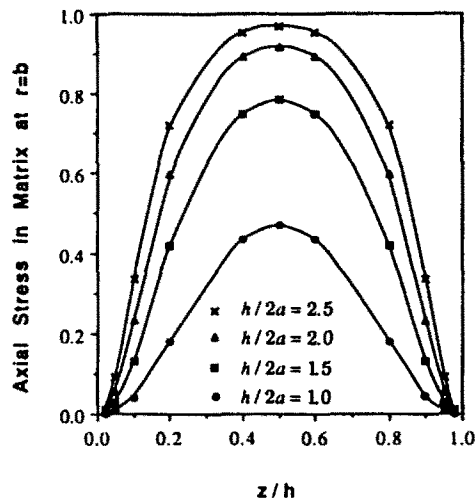

Fig. 10. Normalized axial stress in the matrix at $r = b$ of the SiC/CAS composite for different crack spacings.

REFERENCES

Benthem, J. P. and Koiter, W. T. (1973). Asymptotic approximations to crack problems. In *Mechanics of Fracture 1 : Methods of Analysis and Solutions of Crack Problems* (Edited by G. C. Sih), pp. 131–178. Noordhoff, Leyden.
Bowie, O. L. (1973). Solutions of plane crack problems by mapping technique. In *Mechanics of Fracture 1 : Methods of Analysis and Solutions of Crack Problems* (Edited by G. C. Sih), pp. 1–55. Noordhoff, Leyden.
Collins, W. D. (1962). Some axially symmetric stress distributions in elastic solids containing penny-shaped cracks. *Proc. R. Soc. Lond., Series A* 266, 359–386.
Daniel, I. M., Anastassopoulos, G. and Lee, J.-W. (1989). Experimental micromechanics of brittle-matrix composites. In *Micromechanics : Experimental Techniques* (Edited by W. N. Sharpe Jr.), AMD Vol. 102, ASME, pp. 133–146.

Erdogan, F., Gupta, G. D. and Cook, T. S. (1973). Numerical solution of singular integral equations. In *Mechanics of Fracture I: Methods of Analysis and Solutions of Crack Problems* (Edited by G. C. Sih), pp. 368–425. Noordhoff, Leyden.

Evans, A. G. and Marshall, D. B. (1989). The mechanical behavior of ceramic matrix composites. *Acta Metall.* **37**, 2567–2583.

Krenk, S. (1975). On the use of the interpolation polynomial for solutions of singular integral equations. *Q. Appl. Math.* **32**, 479–484.

McCartney, L. M. (1989). New theoretical model of stress transfer between fiber and matrix in a uniaxially fibre-reinforced composite. *Proc. R. Soc. Lond., Series A* **425**, 215–244.

Nemat-Nasser, S., Keer, L. M. and Parihar, K. S. (1978). Unstable growth of thermally induced interacting cracks in brittle solids. *Int. J. Solids Structures* **14**, 409–430.

Nied, H. F. (1987). Periodic array of cracks in a half plane subjected to arbitrary loading. *J. Appl. Mech. ASME* **54**, 642–648.

Wijeyewickrema, A. C., Keer, L. M., Hirashima, K. and Mura, T. (1991). The annular crack surrounding an elastic fiber in a tension field. *Int. J. Solids Structures* **27**, 315–328.

Wijeyewickrema, A. C. and Keer, L. M. (1991). Matrix fracture in brittle matrix fiber-reinforced composites. *Int. J. Solids Structures* **28**, 43–65.